An adaptive electrodynamic metamaterial for robust absorption of vibration

L. Singleton [1]**, J. Cheer** [1]**, S. Daley** [1]
[1] University of Southampton, Institute of Sound and Vibration Research,
University Road, Southampton, UK
e-mail: **ls2u17@soton.ac.uk**

Abstract

A tuneable elastic metamaterial (EMM) consisting of locally resonant substructures, where the effective bandgap can be controlled to provide optimal attenuation, provides a solution to the issues arising from parametric uncertainty in a structure. The resonance frequency of an inertial electrodynamic actuator can be tuned by connecting a resonant shunt impedance across the terminals. This paper proposes an adaptive electrodynamic metamaterial (AEDMM) unit cell consisting of an array of 12 inertial electrodynamic actuators, each with a dedicated variable impedance shunt. An adaptive tuning method is proposed, based on short-time fourier analysis of the structural velocity, tuning the closed-circuit resonance frequencies of the actuators to the frequency bands with the greatest magnitudes. The system is simulated for a nominal multiple degrees of freedom structure, and for cases of structural uncertainty. The proposed AEDMM is shown to offer greater nominal and considerably greater robust performance compared to an EMM with fixed tuning.

1 Introduction

Locally resonant metamaterials, consisting of distributed resonant unit cells, have been shown to provide narrow-band attenuation of vibration in structures at a scale much smaller than that of the wavelengths involved [1, 2]. Multiple bands of absorption can be achieved using multiple degree-of-freedom (MDOF) resonators [3], or multiple resonators tuned to different frequencies [4]. However, achieving robust absorption of multiple frequencies in the presence of uncertainty is difficult, and tuneable resonators could offer a solution.

Tuneable resonators can be achieved by connecting resonant electronic impedance circuits to electromechanical transducers such as electrodynamic assemblies or piezoelectric transducers, known as shunting [5]. These have the benefit over other methods of variable tuning [6, 7] by being easily translatable to a small scale for integration into a metamaterial, and in the case of electrodynamic actuators, low-cost. A variable shunt impedance can be synthesised digitally and implemented as a voltage filter in conjunction with an analogue voltage controlled current source [8]. However, digital synthetic shunting requires a very high sampling frequency to avoid latency issues, and is not feasible for application to a large array of independently shunted resonators due to the significant computational requirements. A matrix-switched bank of circuits could be designed to allow the selection of discrete tuning frequencies for each resonator on a very small scale, with the only computational cost being setting or computing the tuning frequencies required.

As an alternative to manual tuning of shunted electrodynamic inertial resonators, recent studies have shown that sweeping or switching the tuning frequency of a shunted inertial resonator across a range of frequencies using digital synthetic impedances, can achieve broadband vibration suppression [9]. However, sweeping or switching with no knowledge of the structural response could be less efficient than an adaptive approach, which only switches between frequencies of high magnitude. Adaptive piezoelectric shunt damping has been implemented using digital synthetic shunts to minimise an estimate of the piezoelectric patch strain [10], and to iteratively tune the effective stiffness of a shunted piezo-stack proof-mass resonator to minimise the transmissibility [11]. Piezo-based programmable metamaterials have also been developed [12] but are

yet to integrate adaptive or automated tuning. Piezoelectric patches are only able to exert a bending moment and piezo-stacks have, in general, a small stroke. Therefore, electrodynamic inertial resonators will be more flexible for application to different structures and be able to exert a greater force as they have a larger stroke.

In this study, a novel adaptive electrodynamic metamaterial (AEDMM) is proposed, consisting of an array of 12 inertial electrodynamic actuators connected to independently controlled switching analogue shunt circuits. The adaptive algorithm switches the shunt circuit such that the actuators are tuned to the peaks in the dynamic response of the attached structure. The nominal and robust performance of the proposed system when mounted on a MDOF structure with parametric uncertainty, is evaluated in a simulation study and compared to a fixed-tuning electrodynamic metamaterial (EDMM), which has been tuned to the calculated modal frequencies of the nominal structure alone.

2   Adaptive Metamaterial Design

2.1   Actuator dynamics

There are a number of small form-factor inertial actuators readily available. For this study, the Tectonic Elements TEAX09C005-8 [13] is used because of the low unit cost, and is assumed here to be an ideal, linear system. Figure 1 shows a photo of the actuator and the ideal electromechanical model as a single degree-of-freedom (SDOF) resonator. The mechanical and electrical parameters of this actuator were taken from the data sheet [13] and are: electrical resistance of the coil, $R_{coil} = 8\ \Omega$; electrical inductance of the coil, $L_{coil} = 0.07$ mH; force-factor, $Bl = 1.1$ Tm; moving mass, $m_r = 0.00132$ kg; suspension stiffness, $k_r = 2000$ Nm^{-1}; and damping coefficient, $b_r = 0.03$ Nsm^{-1}.
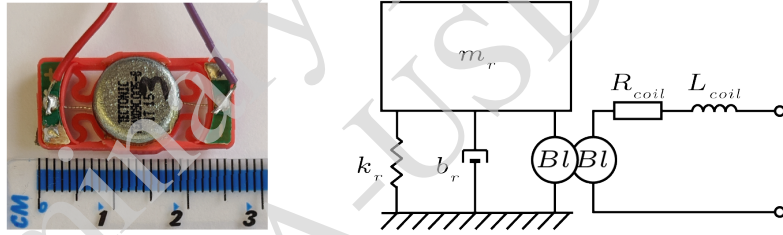

Figure 1: Tectonic Elements TEAX09C005-8 Miniature Audio Exciter (left) and ideal electromechanical representation (right).

2.2   Shunt circuit

Resonant shunt circuits connected to the outputs of an electromechanical transducer can be used to change the resonance frequency of the transducer, allowing it to be 'tuned' to a frequency of choice. The effect of a parallel shunt circuit has been considered in the literature. Turco and Gardonio [9] showed that a resistance and inductance in parallel with the coil present an additional effective damping and stiffness respectively. Following the same derivation, a capacitance can be represented as an additional mass. Figure 2 shows an actuator shunted by parallel resistance R_s, inductance L_s, and capacitance C_s. A negative resistance and inductance are also included to cancel out the impedance of the coil. Also shown in Figure 2 is the equivalent mechanical representation.

Assuming simple harmonic motion, the closed circuit resonance frequency, $f_{r,c}$ of the shunted actuator can be expressed as

$$f_{r,c} = \frac{1}{2\pi}\sqrt{\frac{k_r + \frac{(Bl)^2}{L_s}}{m_r + C_s(Bl)^2}}. \tag{1}$$
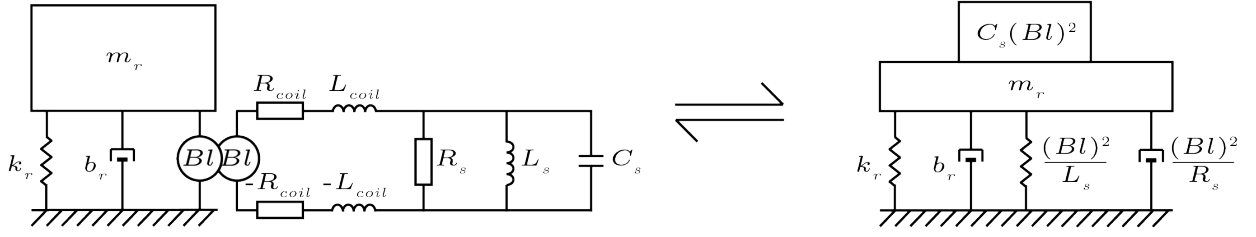
Figure 2: Electromechanical diagram (left) and equivalent mechanical (right) diagram of an ideal shunted electrodynamic inertial actuator.

From Eq. (1) it can be seen that the effective stiffness increases as L_s decreases and the effective mass increases as C_s increases. For simplicity in tuning the resonators, it is assumed that for $f_{r,c} > f_{r,o}$, where $f_{r,o}$ is the open-circuit resonance frequency, the capacitance is switched out of the circuit and for $f_{r,c} < f_{r,o}$ the inductance is switched out of the circuit. The required values of L_s and C_s can therefore be expressed as

$$L_s = \frac{(Bl)^2}{\omega_{r,c}^2 m_r - k_r}; \tag{2}$$

$$C_s = \frac{k_r - \omega_{r,c}^2 m_r}{(Bl)^2 \omega_{r,c}^2}. \tag{3}$$

For a desired damping ratio of ζ, the required R_s can be expressed as

$$R_s = \frac{(Bl)^2}{2\zeta\omega_{r,c} m_r - b_r}. \tag{4}$$

At very low frequencies, R_s can become negative when $b_r > 2\zeta\omega_{r,c} m_r$. To prevent this, the b_r term can be neglected and Eq. (4) becomes

$$R_s = \frac{(Bl)^2}{2\zeta\omega_{r,c} m_r}. \tag{5}$$

This removes the possibility of R_s being negative but the calculated value for R_s cannot accurately produce the specified damping ratio ζ. The actual damping ratio of the shunted resonator will be much higher at low frequencies (for example, for $\zeta = 0.01$, the actual damping ratio at 10 Hz is 0.19 and at 100 Hz is 0.03). Because of this, attenuation at low frequencies will likely be reduced.

2.3 Adaptive algorithm

The proposed adaptive tuning algorithm uses a 'greatest magnitude' frequency selection approach. This involves the frequency response of the structure and the 12 highest magnitude frequency bins being taken as the tuning frequencies. A logarithmic frequency vector is used for the frequency analysis in order to better distribute the frequency points with relation to the bandwidth of the modes. The algorithm is set out step-by-step below.

3 Simulation Study

3.1 Simulation method

A nominal three degree-of-freedom, mass-spring-damper system with a fixed base is simulated, with the AEDMM consisting of 12 electrodynamic resonators connected to the free, top mass as shown in Figure 3. The total mass of the structure is set such that the mass of the AEDMM equates to approximately 10%

Algorithm 1: adaptive tuning

Input: $\dot{w}[n]$

Output: R_s, L_s, C_s

  1: Calculate frequency domain response using a logarithmically distributed FFT over the previous NFFT samples.

  2: Sort frequency vector in descending order of frequency response magnitude.

  3: Truncate frequency vector to first 12 (corresponding to the 12 highest magnitudes).

  4: Calculate required R_s, L_s and C_s values to achieve selected tuning frequencies and damping ratio.

  5: Implement new component values.

  6: Wait n_{update} samples.

  7: Repeat

---

of the structure. The structural mass is divided equally between masses $m_{1,\,2\;and\;3}$. The stiffness values $k_{1,\,2\;and\;3}$ are set to provide three modes of vibration within the frequency range of 10-500 Hz. All structural damping is modelled with a viscous damping coefficient, b of 0.1 Nsm^{-1}. The disturbance force consists of band-limited white noise and is applied to m_1. All simulations are carried out using MATLAB/Simulink and the Simscape library of mechanical and electrical component blocks, with a sampling frequency of 1 kHz and duration of 60 s. The desired damping ratio of the resonators, ζ is set at 0.01, however as discussed in section 2.2 the actual damping ratio achieved will vary with frequency and be approximately 0.2 at 10 Hz.
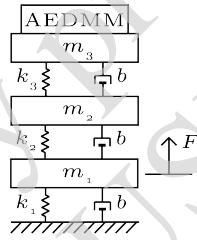

Figure 3: Structure and AEDMM for simulation.

For practical reasons, sensing of the structural response is carried out at the same location as the AEDMM so that components can be contained within one housing. Initial simulations showed that the velocity of the top mass was sufficient to capture all three modes of the structure and the adaptive tuning did not result in any enhancement in the response of any of the three masses. It was therefore concluded that the velocity of the top mass can be used as the structural feedback for the adaptive algorithm.

3.2 Selection of adaptive algorithm parameters

As the adaptive algorithm selects the tuning frequencies based on the frequency bins of the FFT, the length of the FFT (NFFT) will have a strong influence on which points are selected, and the rate at which the algorithm updates the component values (n_{update}) may also affect the performance of the AEDMM. Figure 4 shows the convergence of the broadband attenuation of the kinetic energy of the top mass, $E_{k,\,atten}$ as a contour plot for different values of NFFT and n_{update}. For short update rates ($< 2^7$ samples) the response shows instability (NaN) resulting in a massive increase in energy in the system. This could possibly be due to the introduction of transients when the inductor and capacitor branches of the shunt switch in and out in quick succession. There could also be an element of resonance in the electronic circuit contributing to this instability. From this convergence study the optimal configuration is shown to be NFFT = 512 and n_{update} = 256, which is carried forward to the remainder of the simulation study.
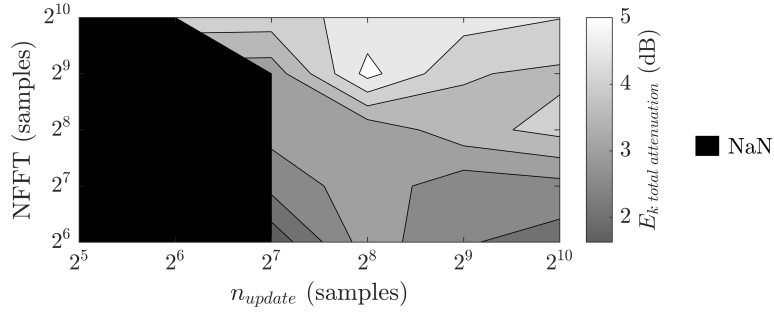
Figure 4: Contour plot showing the attenuation in the kinetic energy provided by the AEDMM for different FFT lengths and update rates. The black area indicates where the response is unstable.

3.3 Nominal Performance

The simulation is run for three cases: the structure alone; the structure with a fixed-shunt EDMM, distributing the resonance frequencies of the actuators equally between the three modal frequencies of the structure; and the structure with the proposed AEDMM. Figure 5 shows the magnitude and phase of the mobility frequency response function (FRF), $Y(j\omega)$ of the top mass in each case. It can be seen how the fixed-tuning achieves attenuation of the second and third modes but causes a 'splitting' of the peak. The AEDMM also achieves attenuation of these modes, but results in a smoother response around the second mode. The AEDMM achieves an $E_{k,\,atten}$ of 4.3 dB compared to just 1.7 dB for the fixed tuning. The AEDMM also does not split the third mode, but appears to cause a shift and reduction in amplitude. Neither approach achieves significant attenuation in the first mode. It is hypothesised that this is down to the increased damping of the resonator at low frequencies as discussed in Section 2.2.
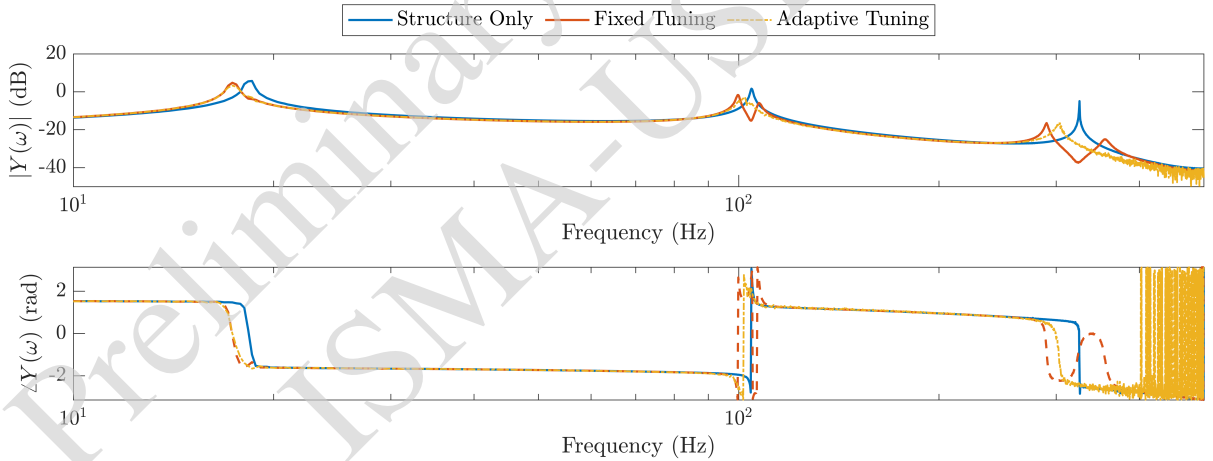

Figure 5: Magnitude (top) and phase (bottom) of the mobility FRF of m_3, with the structure only, with a fixed-tuning EDMM and with the proposed AEDMM.

The selection of tuning frequencies over time is shown in Figure 6, and it can be seen that the third mode is not selected as a tuning frequency at any point. The added mass and damping of the resonators alone has caused the shift and attenuation of the third mode that was shown in Figure 5, which is sufficient to prevent the selection of this frequency.

3.4 Robust Performance

In practical systems, shifts in the resonance frequencies of the structure cause the effectiveness of fixed-tuning resonators to be limited, whereas the AEDMM should still attenuate the highest magnitude points in
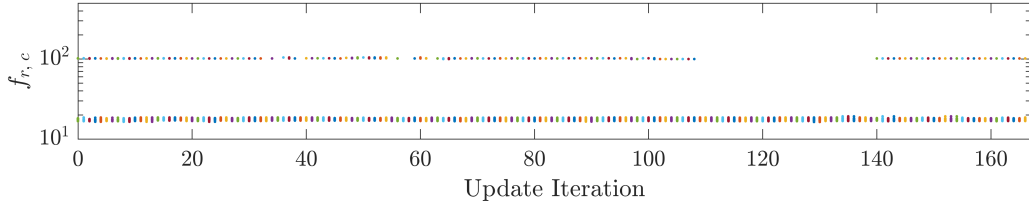
Figure 6: Frequencies selected by the adaptive algorithm over the duration of the simulation.

the frequency response and provide higher robustness to parametric uncertainty in the structure. To investigate this, 50 additional structures based on that shown in Figure 3 are simulated, with parametric variation in the stiffness values. The resulting mean, standard deviation, minimum, and maximum values of the total attenuation in the kinetic energy are shown in Figure 7. From these results it can be seen that the adaptive method achieves approximately 3 dB improvement in the mean $E_{k,\,atten}$, along with large improvements in the minimum and maximum values. The standard deviation (σ) of the adaptive method is marginally higher than the fixed tuning, but the minimum and maximum show a wider range so this is to be expected. These results show clear support for the hypothesis that the AEDMM is significantly more robust to changes in the structure.
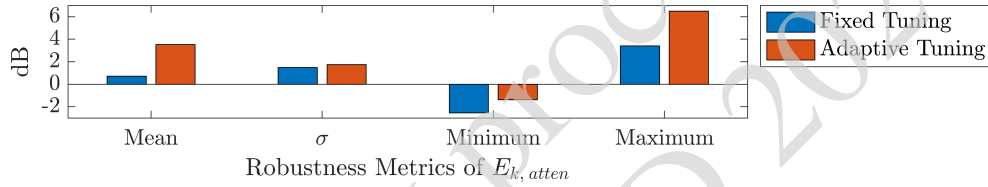

Figure 7: Robustness metrics (mean, standard deviation (σ), minimum and maximum) of $E_{k,\,atten}$ for a range of structural parametric uncertainty, with a fixed-tuning EDMM vs. the proposed AEDMM.

The minimum attenuation for the AEDMM is negative, which equates to a gain. To explain this, Figure 8 shows the mobility FRF for four cases: plots A and B show two structures with relatively small deviations from the nominal; plot C shows the mobility FRFs of the structure which achieved the minimum attenuation for the AEDMM and plot D for the maximum attenuation. From plot C it can be deduced that the overall gain in kinetic energy is caused by the downward shift and enhancement of the first mode which cannot be controlled by either approach, but with the adaptive tuning still outperforming the fixed tuning.
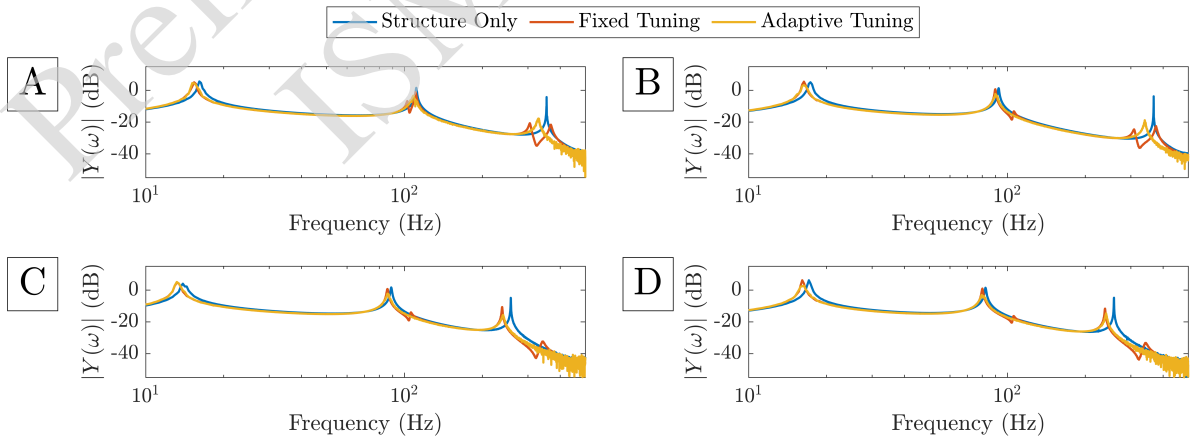

Figure 8: Magnitude of the mobility FRF of m_3, with the structure only, with a fixed-tuning EDMM and with the proposed AEDMM for selected cases of parametric uncertainty. A and B: similar to nominal structure, C: structure where the minimum $E_{k,\,atten}$ was achieved by the AEDMM, D: structure where the maximum $E_{k,\,atten}$ was achieved by the AEDMM.

4 Conclusions

This study has proposed an adaptive electrodynamic metamaterial (AEDMM) for the absorption of vibration in an uncertain structure, consisting of an array of 12 electrodynamic inertial actuators with variable shunt impedances. The AEDMM has been shown to achieve greater attenuation in kinetic energy for a nominal structure when compared to a fixed-tuning EDMM, and greater robustness to structural uncertainty.

Acknowledgements

References

[1] P. F. Pai, H. Peng, and S. Jiang, "Acoustic metamaterial beams based on multi-frequency vibration absorbers," *International Journal of Mechanical Sciences*, vol. 79, pp. 195–205, 2014.

[2] X. W. Yang, J. S. Lee, and Y. Y. Kim, "Effective mass density based topology optimization of locally resonant acoustic metamaterials for bandgap maximization," *Journal of Sound and Vibration*, vol. 383, pp. 89–107, nov 2016. [Online]. Available: https://www.sciencedirect.com/science/article/pii/S0022460X16303522{#}s0025

[3] H. Peng, P. Frank Pai, and H. Deng, "Acoustic multi-stopband metamaterial plates design for broadband elastic wave absorption and vibration suppression," *International Journal of Mechanical Sciences*, vol. 103, pp. 104–114, nov 2015. [Online]. Available: https://www.sciencedirect.com/science/article/pii/S0020740315003136

[4] H. Peng and P. Frank Pai, "Acoustic metamaterial plates for elastic wave absorption and structural vibration suppression," *International Journal of Mechanical Sciences*, vol. 89, pp. 350–361, dec 2014. [Online]. Available: https://www.sciencedirect.com/science/article/pii/S002074031400321X

[5] B. Yan, K. Wang, Z. Hu, C. Wu, X. Zhang, B. Yan, K. Wang, Z. Hu, C. Wu, and X. Zhang, "Shunt Damping Vibration Control Technology: A Review," *Applied Sciences*, vol. 7, no. 5, p. 494, may 2017. [Online]. Available: http://www.mdpi.com/2076-3417/7/5/494

[6] L. M. Miller, P. Pillatsch, E. Halvorsen, P. K. Wright, E. M. Yeatman, and A. S. Holmes, "Experimental passive self-tuning behavior of a beam resonator with sliding proof mass," *Journal of Sound and Vibration*, vol. 332, no. 26, pp. 7142–7152, dec 2013. [Online]. Available: https://www.sciencedirect.com/science/article/abs/pii/S0022460X13006883

[7] S. Sun, H. Deng, J. Yang, W. Li, H. Du, G. Alici, and M. Nakano, "An adaptive tuned vibration absorber based on multilayered MR elastomers," *Smart Materials and Structures*, vol. 24, no. 4, p. 045045, apr 2015. [Online]. Available: http://stacks.iop.org/0964-1726/24/i=4/a=045045?key=crossref.ce9c8952db7ce2e8d2fe501a1f517db6

[8] J. Nečásek, J. Václavík, and P. Marton, "Digital synthetic impedance for application in vibration damping," *Review of Scientific Instruments*, vol. 87, no. 2, p. 024704, feb 2016. [Online]. Available: http://aip.scitation.org/doi/10.1063/1.4942085

[9] E. Turco and P. Gardonio, "Sweeping shunted electro-magnetic tuneable vibration absorber: Design and implementation," *Journal of Sound and Vibration*, 2017.

[10] A. J. Fleming and S. O. R. Moheimani, "Adaptive piezoelectric shunt damping," *Smart Materials and Structures*, vol. 12, no. 1, pp. 36–48, feb 2003. [Online]. Available: http://stacks.iop.org/0964-1726/12/i=1/a=305?key=crossref.383f43d134224114118b53cfe884605c

[11] M. Kodejška, P. Mokrý, V. Linhart, J. Václavik, and T. Sluka, "Adaptive vibration suppression system: An iterative control law for a piezoelectric actuator shunted by a negative capacitor," *IEEE Transactions on Ultrasonics, Ferroelectrics, and Frequency Control*, vol. 59, no. 12, pp. 2785–2796, 2012.

[12] K. Yi, G. Matten, M. Ouisse, E. Sadoulet-Reboul, M. Collet, and G. Chevallier, "Programmable meta-materials with digital synthetic impedance circuits for vibration control," *Smart Materials and Structures*, vol. 29, no. 3, p. 035005, jan 2020.

[13] Tectonic Audio Labs, "Tectonic TEAX09C005-8 Data Sheet." [Online]. Available: https://www.tectonicaudiolabs.com/product/teax09c005-8/?id=product-797